Folding Mechanism of Ketosteroid Isomerase from *Comamonas testosteroni*†

Do-Hyung Kim,‡ Do Soo Jang, Gyu Hyun Nam, and Kwan Yong Choi*

Division of Molecular and Life Sciences, Center for Biofunctional Molecules, Pohang University of Science and Technology, Pohang, 790-784, South Korea

Received August 14, 2000; Revised Manuscript Received February 5, 2001

ABSTRACT: Ketosteroid isomerase (KSI) from *Comamonas testosteroni* is a homodimeric enzyme with 125 amino acids in each monomer catalyzing the allylic isomerization reaction at rates comparable to the diffusion limit. Kinetic analysis of KSI refolding has been carried out to understand its folding mechanism. The refolding process as monitored by fluorescence change revealed that the process consists of three steps with a unimolecular fast, a bimolecular intermediate, and most likely unimolecular slow phases. The fast refolding step might involve the formation of structured monomers with hydrophobic surfaces that seem to have a high binding capacity for the amphipathic dye 8-anilino-1-naphthalenesulfonate. During the refolding process, KSI also generated a state that can bind equilenin, a reaction intermediate analogue, at a very early stage. These observations suggest that the KSI folding might be driven by the formation of the apolar active-site cavity while exposing hydrophobic surfaces. Since the monomeric folding intermediate may contain more than 83% of the native secondary structures as revealed previously, it is nativelike taking on most of the properties of the native protein. Urea-dependence analysis of refolding revealed the existence of folding intermediates for both the intermediate and slow steps. These steps were accelerated by cyclophilin A, a prolyl isomerase, suggesting the involvement of a cis-trans isomerization as a rate-limiting step. Taken together, we suggest that KSI folds into a monomeric intermediate, which has nativelike secondary structure, an apolar active site, and exposed hydrophobic surface, followed by dimerization and prolyl isomerizations to complete the folding.

Δ^5-3-Ketosteroid isomerase (KSI)[1] from *Comamonas testoseroni* is an enzyme catalyzing the allylic isomerization of a variety of 3-oxo-Δ^5-steroids to their conjugated Δ^4-isomers by an intramolecular transfer of the 4β-proton to the 6β-position via an enolate intermediate (*1*). KSI is a homodimeric enzyme with 125 amino acids in each monomer (*2*). Recent determinations of the X-ray crystal structures as well as the NMR solution structures revealed that KSI consists of a six-stranded β-sheet and three α-helices in each monomer (*3, 4*) (Figure 1). Each monomer forms one complete active site made of the residues from the same monomer, not from the partner monomer. The active-site cavity is hydrophobic so as to be effective for binding steroid substrates. The monomers interact extensively with each other over a narrow and long patch of β-sheet of each monomer. The same tertiary fold has been identified in scytalone dehydratase (*6*) and nuclear transport factor-2 (*7*), distinct in their functions from that of KSI. The homologous isozyme from *Pseudomonas putida* biotype B with 34% amino acid identity also exhibited the same tertiary fold as *C. testosteroni* KSI (*8*). It is likely to be the general design of the active-site cavity that determines this common tertiary fold (*9*). Whether a general folding mechanism is applicable for these proteins would be a very interesting question.

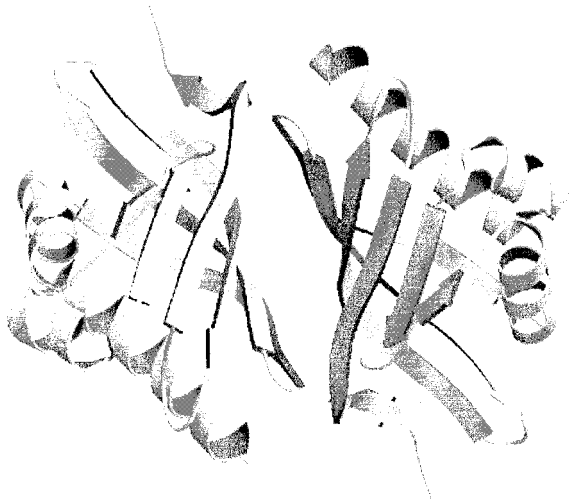

FIGURE 1: Ribbon diagram of the three-dimensional structure of *C. testosteroni* KSI dimer. The each monomer consists of three α-helices and six β-strands. The program Molscript (*5*) was used for drawing the figure.

As a small dimeric protein, KSI provides a good model system to understand the folding mechanism of dimeric proteins. This protein is highly expressed in *Escherichia coli* and conveniently purified utilizing an affinity column (*10, 11*). In addition, the availability of the NMR solution structures as well as the high-resolution crystal structures is

† This work was supported by a grant from Korea Science and Engineering Foundation, and in part by the Brain Korea 21 Project.

* To whom correspondence should be addressed. Tel: 82-54-279-2295. Fax: 82-54-279-2199. E-mail: kchoi@postech.ac.kr.

‡ Current address: Whitehead Institute for Biomedical Research, Nine Cambridge Center, Cambridge, MA 02142.

[1] Abbreviations: KSI, ketosteroid isomerase; ANS, 8-anilino-1-naphthalenesulfonate; d-equilenin, *d*-1,3,5(10),6,8-estrapentaen-3-ol-17-one.

10.1021/bi0019139 CCC: $20.00
Published on Web 03/24/2001

very valuable in analyzing the folding mechanism in molecular detail. Recent studies on the equilibrium unfolding of KSI revealed that the interface interactions are crucial for maintaining the tertiary structure (*12*). The folding of KSI was determined to be reversible and follow a simple two-state mechanism consisting of only the native dimer and the unfolded monomer without any thermodynamically stable intermediates. The folding mechanism seems to be much more complicated than the two-state model where unstructured monomers collide to form the native state in a single phase. The KSI folding appears to begin with the internalization of the active-site tyrosine residues to generate a partially folded monomer. The partially folded monomers will meet each other to form a dimeric intermediate, which is then followed by intramolecular events for complete formation of the KSI structure. This folding mechanism is consistent with those of such dimeric proteins as Trp repressor (*13*, *14*), glutathione transferase A1-1 (*15*), and triosephosphate isomerase (*16*, *17*) since a monomeric folding intermediate occurs prior to dimerization. In contrast, P22 Arc repressor provides a different example in which any monomeric folding intermediate does not exist during refolding (*18*).

The characterization of folding intermediates is essential for understanding the folding mechanism of KSI. The amphipathic fluorescence probe 8-anilino-1-naphthalenesulfonate (ANS) is expected to detect the hydrophobic patch transiently generated on the surface of the monomeric folding intermediate (*19*, *20*). The apolar active-site formation may be monitored by taking advantage of steroid binding to the active site since KSI binds steroids at the diffusion-controlled rate. When KSI binds d-equilenin, a reaction intermediate analogue, the fluorescence intensity of the steroid decreases due to the quenching effects by the interaction between the steroid and the enzyme (*21*). Urea dependence analysis of the refolding kinetics is important to dissect the folding mechanism since it can provide evidence for the existence of folding intermediates for the respective refolding steps.

In this study, the folding mechanism of KSI from *C. testosteroni* has been investigated by use of different probes to detect the structural changes. The ANS binding studies during refolding revealed that the monomeric folding intermediate might have the hydrophobic surface to bind ANS transiently. Fluorescence quenching of equilenin that binds to the KSI active site was utilized to monitor the active-site formation. The kinetic traces for refolding were analyzed at different urea concentrations to dissect the folding mechanism and rate-limiting reactions for the respective refolding step. The intermediate and slow phases were accelerated by a prolyl isomerase, suggesting the involvement of proline isomerizations as a rate-limiting step in these phases.

EXPERIMENTAL PROCEDURES

Reagents and Experimental Conditions. Chemicals for buffer solutions, deoxycholate, ANS, and ultrapure urea were purchased from Sigma. Equilenin was purchased from Steraloids. Cyclophilin A was obtained from Roche Molecular Biochemicals. The temperature was maintained at 25 °C for all experiments unless specified otherwise. The protein concentration was determined on the basis of the difference spectrum change at 295 nm (*22*). The enzyme concentration is reported for monomer unless otherwise specified.

Protein Source and Purification. The wild-type KSI from *C. testoseroni* was overexpressed in *E. coli* BL21(DE3) containing pKSI-TI (*3*), an expression vector carrying the *C. testosteroni* KSI wild-type gene, and purified to homogeneity by deoxycholate affinity chromatography and Superose 12 gel filtration chromatography according to the methods reported previously (*11*). The purity of the protein was confirmed by the presence of a single band on an SDS−polyacrylamide gel stained with Coomassie blue.

Kinetic Analysis of Refolding. The kinetic trace of the KSI refolding was monitored by use of a stopped-flow instrument (Bio-logic SFM-4/QS). Fifty microliters of the denatured KSI dissolved in a denaturing buffer containing 20 mM potassium phosphate, pH 7.0, and 7 M urea was mixed with 500 μL of 20 mM potassium phosphate at pH 7.0. The final protein and urea concentrations were 3 μM and 0.64 M, respectively, in the refolding condition. For the spectroscopic measurements, a cuvette (Bio-logic, FC-20) with a 2 mm path length was used, and a specially designed mixer (Bio-logic, HDS) was implemented to enhance the mixing efficiency with urea. During refolding, the fluorescence passed through the 295 nm cutoff filter (Oriel) was measured after the excitation at 275 nm. The light source was a Xe/Hg lamp. The dead time of the instrument was 8 ms. Refolding kinetics were analyzed under various concentrations of urea (0−3.5 M). Refolding catalyzed by peptidyl-prolyl isomerase was investigated with increasing amounts of cyclophilin A (0−3 μM) in the refolding buffer. The obtained refolding trace was analyzed to obtain the refolding rate constants by fitting the data to the equation:

$$F_t = F_\infty + \sum F_i[1 - \exp(-k_i t)] \quad (1)$$

where F_t is the signal at time t, F_∞ is the signal of the final state, F_i is the amplitude of the kinetic phase, and k_i is the rate constant for refolding. Data fitting was performed using the program Kaleidagraph version 2.6 (Abelbeck Software).

ANS Binding Experiments. The KSI refolding was analyzed in the presence of ANS. The denatured protein in 7 M urea was induced to refold according to the procedure as described above except that the refolding buffer contained 50 μM ANS. The fluorescence passed through a 400 nm cutoff filter (Oriel) was monitored after the excitation at 350 nm. The ANS binding to the native and denatured states of KSI was also analyzed by obtaining the emission fluorescence spectra of ANS by use of a spectrofluorometer (Shimazhu 5300). With the excitation wavelength of 350 nm, the emission spectrum was monitored in the range from 400 to 650 nm. The bandwidths for the excitation and emission wavelengths were 5 and 1.5 nm, respectively. The step resolution and the integration time were 1 nm and 1 s, respectively. The denatured protein was obtained by incubating the protein in the buffer containing 20 mM potassium phosphate, pH 7.0, and 7 M urea.

Equilenin Binding Experiments. The equilenin binding kinetics were monitored during the KSI folding process by utilizing the quenching effect of equilenin when KSI binds equilenin (*21*). The KSI refolding was induced in the presence of 3 μM equilenin. Fluorescence emitted through a 335 nm cutoff filter was monitored after excitation at 310 nm. Four different protein concentrations, 0.5, 1, 3, and 5 μM, were tried to analyze the dimerization step in the folding

process. The trace was fitted to exponential functions according to eq 1. The baseline of the free equilenin fluorecence was also monitored to correct the absolute change of the fluorescence.

RESULTS

Identification of ANS Binding Intermediate. Previous analysis revealed that the KSI refolding could be explained by three kinetic phases (*12*). The fast phase was followed by a bimolecular intermediate phase and most likely a unimolecular slow phase. This refolding kinetic analysis led to the speculation that a monomeric folding intermediate might occur with exposed hydrophobic surface that will be buried during dimerization. The amphipathic fluorescent probe ANS was utilized to monitor the formation of this hydrophobic surface during protein folding. Prior to this, it was investigated whether ANS binds to the native state or the unfolded state of KSI by analyzing the spectral change of ANS. The free ANS exhibits the emission fluorescence maximum at 517 nm when excited at 350 nm. Upon binding to native KSI, the ANS fluorescence was marginally enhanced with a 5 nm blue shift in the maximum wavelength (Figure 2A). This suggests that the native state binds ANS weakly. The denatured state enhanced the ANS fluorescence intensity by approximately 2-fold while shifting the maximum wavelength by 5 nm, implying that the denatured state might have a hydrophobic surface to bind ANS more strongly than the native state.

To identify the generation of hydrophobic clusters during refolding, the fluorescence change of ANS was monitored during KSI refolding in the presence of ANS. There was an initial rapid enhancement of fluorescence, and the increase continued for about 100 ms (Figure 2B). The enhancement in fluorescence was followed by a rapid decrease. It is not clear whether the unusual rapid decrease of the ANS signal can be any of the kinetic phases detected by protein fluorescence changes. Rather, the decrease might be related to desorption of ANS from the denatured species that binds ANS relatively better than the native state (Figure 2A). Following the rapid decrease, the ANS signal was marginally increased and slowly decreased. It seems likely that the increase of the ANS signal might be related to preferential binding of ANS to exposed hydrophobic patches in the partially folded and loosely packed intermediate. This result is consistent with the exposure of hydrophobic surface that allows the interaction with ANS prior to dimerization. The slow decrease of the ANS fluorescence signal might reflect desorption of ANS probably as a consequence of occlusion of the hydrophobic surface upon structural rearrangements.

The protein fluorescence change monitored during the refolding in the presence of ANS exhibited almost the same signal pattern as that of the ANS signal (Figure 2C). This suggests that the ANS binding affected the protein fluorescence signal. This could arise from the spectral overlap of ANS and protein. In addition, however, it is clear that the kinetics of the refolding process are substantially altered by the presence of ANS. This could indicate that the presence of ANS is affecting the structural changes occurring in the protein. The signal after 0.4 s could be analyzed well by two kinetic phases with rate constants of 0.13 and 0.013 s^{-1}, which are comparable to those of the intermediate and slow phases, respectively, obtained in the absence of ANS. However, their relative amplitudes were significantly affected, in which the amplitude of the slow phase was increased 6-fold relative to that of the intermediate one. This might reflect that ANS does not affect the overall kinetics significantly but it does differentially affect the fluorescence signals of the intermediate and slow phases. The large change in the relative amplitudes could be due to our ignorance of

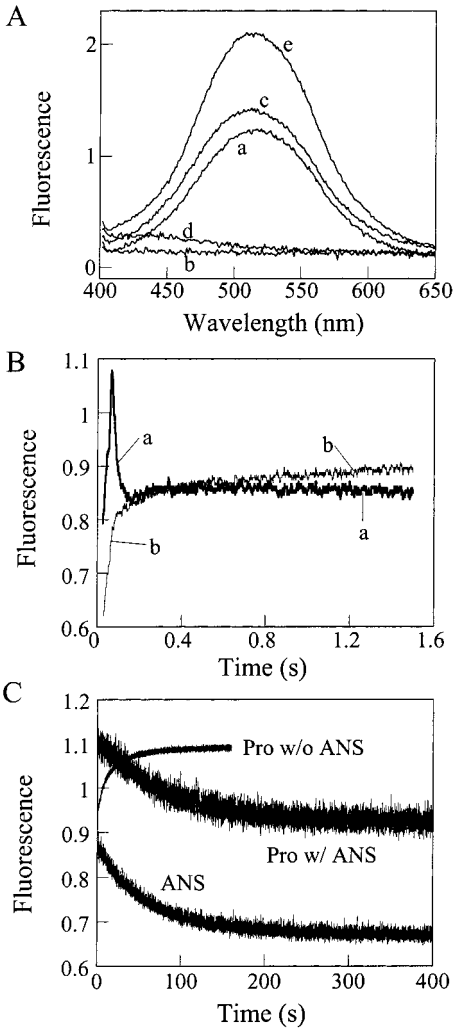

FIGURE 2: ANS binding studies to monitor the generation of hydrophobic surfaces during KSI refolding. (A) ANS fluorescence spectra obtained when 50 μM ANS was incubated with 3 μM KSI at different folding states. The excitation wavelength was 350 nm. The protein was dissolved in 20 mM potassium phosphate, pH 7.0, with or without 7 M urea for the native or denatured protein, respectively. Each spectrum represents free ANS (a), the native state (b), the native state + ANS (c), the denatured state (d), and the denatured state + ANS (e), respectively. (B) ANS fluorescence change monitored during KSI refolding (a). 3 μM KSI was induced to refold in the presence of ANS by using the Bio-logic mixing apparatus. The sample was excited at 350 nm, and the fluorescence intensity passed through a 400 nm cutoff filter was monitored. The kinetic trace of KSI refolding obtained by monitoring the fluorescence intensity passed through a 295 nm cutoff filter after excitation at 275 nm was also shown for comparison (b). (C) Effect of ANS on protein refolding. The protein refolding process was monitored in the presence of ANS (Pro w/ ANS) and compared to that obtained in the absence of ANS (Pro w/o ANS). The sample was excited at 275, nm and the fluorescence passed through a 295 nm cutoff filter was monitored. For comparison, the ANS signal (ANS) was drawn for a long time scale.

the signal prior to 0.4 s in interpretation, in which the signal is too complicated to obtain the reliable kinetic values.

Detection of Equilenin Binding Conformation. One approach that would be applicable for KSI folding analysis may involve the utilization of equilenin binding. Equilenin binds to the active site of the native KSI to form hydrogen bonds with Tyr14 and Asp99 (*23*). The hydrogen bonds as well as the hydrophobic environment of the active site may contribute to the decrease of equilenin fluorescence (*21*). Thus, monitoring of the equilenin fluorescence quenching during refolding may reflect the formation of the active site which can bind the steroid. The excitation wavelength was 310 nm, and the fluorescence passed through a 335 nm cutoff filter was monitored to analyze the extent of equilenin binding to KSI during refolding. The choice of these wavelengths could allow us to avoid any disturbance that may originate from the quenching of intrinsic fluorescence of the protein upon equilenin binding. The fluorescence significantly decreased at a very early stage. The abrupt fluorescence quenching occurred before 0.35 s, which accounted for approximately 40% of the total amplitude (Figure 3). The signal prior to 0.35 s was hard to analyze due to severe noise peaks. This fluorescence quenching suggests that the hydrophobic active site might form rapidly at a very early stage. The rapid fluorescence quenching also implies that KSI binds equilenin very rapidly due to the favorable hydrophobic environment of the KSI active site. After the abrupt decrease in fluorescence, the fluorescence decreased slowly with rate constants of approximately 0.21 and 0.01 s^{-1} for the intermediate and slow phases, respectively, at 3 μM KSI. These rate constants were comparable to those of the intermediate and slow phases observed by the intrinsic fluorescence change of KSI. This result implies that the dimerization might contribute to the formation of the hydrophobic active site. Since the K_D for equilenin is approximately 2 μM (*24*), the concentration of equilenin bound to KSI would be approximately 1.4 μM when the protein concentration was 3 μM.

Urea Dependence of Refolding. To dissect the three kinetic phases, the kinetic behavior of each refolding step was analyzed at different urea concentrations. The refolding process could be divided into the fast, intermediate, and slow phases over the overall urea range as described previously for refolding at 0.64 M urea (*12*). When the rate constant for refolding was plotted in logarithmic scale against urea concentration, the refolding rate for the fast phase decreased in the 0−3.5 M urea range without any evidence of deviation from linearity (Figure 4A). The rate constants for the intermediate and slow phases also decreased as the urea concentration increased, but the slope was deviated from linearity in the manner that at low concentrations below 1.5 M urea the rate constants were more weakly dependent upon urea. This suggests that the rate-limiting step may change under strongly refolding conditions. Thus, the intermediate and slow steps may be governed by more than one refolding step.

The amplitudes of the refolding phases were also changed depending upon the final urea concentration. The relative amplitude of the fast phase decreased as the urea concentration increased. The intermediate phase accounted for a larger portion of amplitude at higher urea concentrations, but the amplitude remained constant in the 2.3−3 M urea range. The

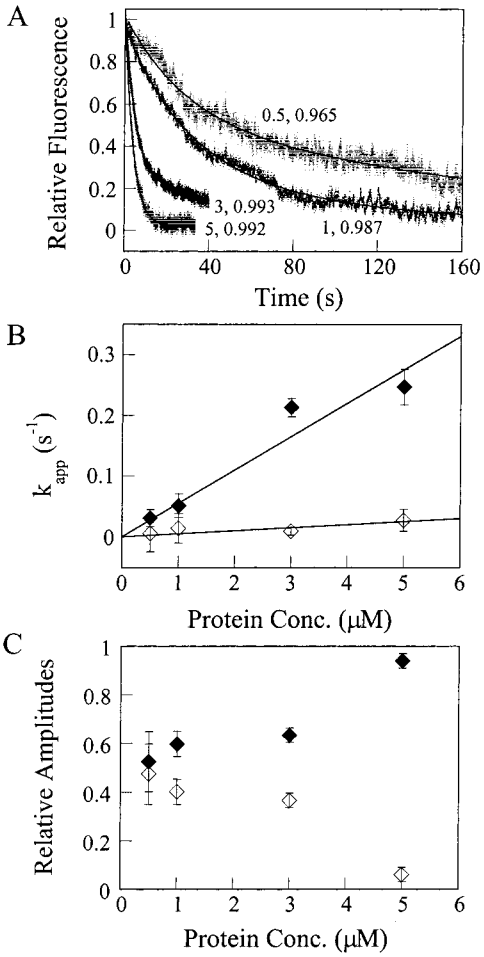

FIGURE 3: Equilenin fluorescence quenching during KSI refolding. (A) Kinetic traces of the equilenin fluorescence change obtained at four different protein concentrations, 0.5, 1, 3, and 5 μM. The equilenin concentration was 3 μM. The mixing conditions are the same as described under Experimental Procedures. The trace was fitted by two exponential functions. The numbers represent the protein concentration and R^2, respectively. (B) Dependence of rate constants and (C) amplitudes on protein concentration. The rate constants and amplitudes for the intermediate (◆) and slow phases (◇) were plotted against the protein concentration. The lines represent the linear relationship between the rate constant and the protein concentration.

relative amplitude of the slow phase decreased slowly and then increased at urea concentrations higher than 2.5 M. The amplitudes for the refolding events indicate that the fast, intermediate, and slow phases account for 50%, 20%, and 30% of the total amplitude change at 0.55 M urea, respectively (Figure 4B). This variation in the amplitudes of the three refolding phases as a function of the final urea concentration may reflect the stability of the folding intermediates. The decrease in the relative amplitude of the fast phase and the corresponding increase in the amplitude of the intermediate phase suggest that the monomeric intermediate is relatively destabilized at higher urea concentration.

The urea dependence of the intermediate refolding rate parallels that of the slow phase in the range between 0 and 1.5 M urea. Similar dependence was observed between 1.5 and 3 M urea. This observation suggests similar compactness or solvent accessibility of the transition states for these phases. Comparison of $m_f^{\ddagger}$ obtained from the kinetic studies over the 1.8−3 M urea range and m obtained from the

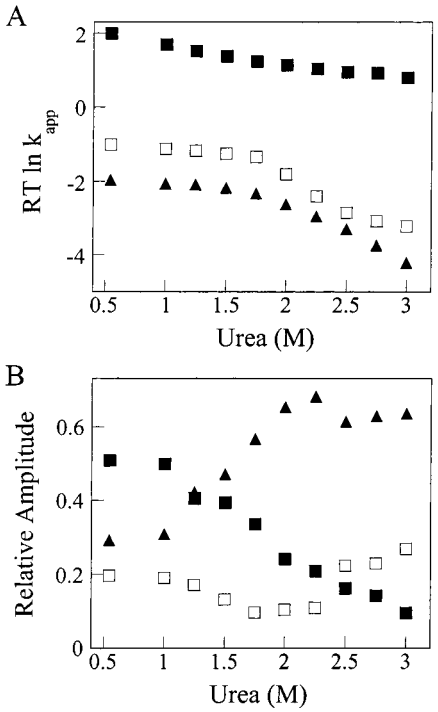

FIGURE 4: Urea dependence of the refolding rate constants and amplitudes. (A) The refolding rate constants for the fast (■), intermediate (□), and slow phases (▲) were plotted in logarithmic scale against the final urea concentration. (B) The relative amplitudes of the total fluorescence change of the fast, intermediate, and slow phases were displayed against the urea concentration. 3 μM KSI was refolded in the indicated urea concentration. The fluorescence change was analyzed by use of eq 1 to obtain the rate constants and amplitudes.

equilibrium unfolding studies suggests that the refolding rates accounted for about 18%, 60%, and 38% of the urea dependence of the equilibrium constant for the fast, intermediate, and slow phases, respectively. This indicates that a considerable amount of hydrophobic surface might be buried during the intermediate step.

cis-trans Isomerization in KSI Refolding. KSI has five proline residues per subunit, and the peptide bond preceding Pro39 is in a cis configuration in the native state (*25*). The cis peptide bond, located at the end of strand 1, is conserved for *P. putida* KSI. Since Asp38 is the catalytic residue, the cis peptide bond seems to be important for maintaining the correct conformation of the active site or for the right orientation of Asp38 for efficient catalysis. Cyclophilin A, a peptidyl-prolyl isomerase, was utilized to determine whether any of the refolding phases of KSI are limited by proline isomerization. The effect of increasing concentrations of cyclophilin A on the refolding rates is shown in Figure 5. The rate constant of the fast phase was unaffected while the rate constants for the intermediate and slow phases were accelerated over the range of 0−3 μM cyclophilin. The intermediate and slow phases are thus kinetically coupled with prolyl isomerizations, which is consistent with the expectation that these steps might involve more than one refolding step as revealed from the urea dependence analysis as described above. The higher dependence on cyclophilin A observed for the slow step than for the intermediate step reflects that the slow step is relatively more affected by proline isomerizations.

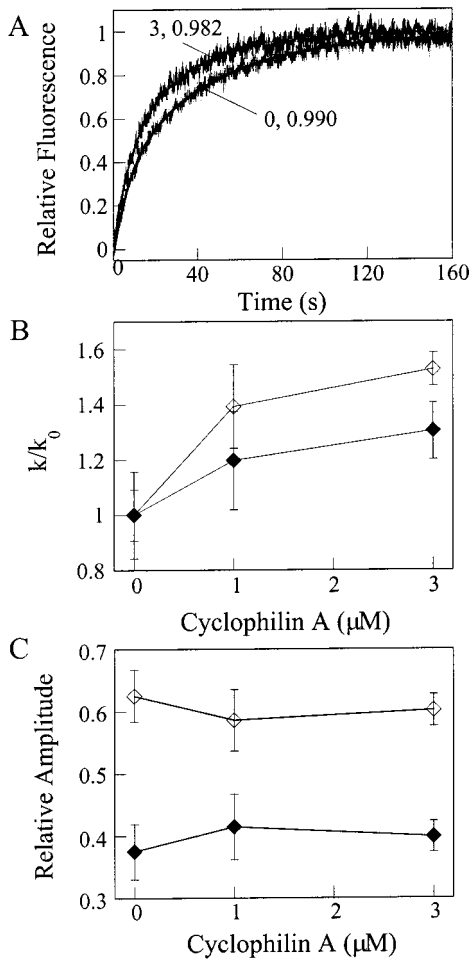

FIGURE 5: Catalytic effect of cyclophilin A on the refolding kinetics. (A) The kinetic trace of KSI refolding monitored by the fluorescence change in the presence of cyclophilin A at different concentrations, 0, 1, and 3 μM. The protein concentration was 3 μM. The *y*-axis represents the relative fluorescence change obtained by taking the fluorescence at 0 and ∞ as 0 and 1, respectively. The numbers represent the cyclophilin A concentration and R^2, respectively. (B) Dependence of the apparent rate constants on the concentration of cyclophilin A. The rate constants for the intermediate (◆) and slow phases (◇) were plotted against the concentration of cyclophilin A. The ratio k/k_0 was calculated from the refolding rate in the presence (k) and the absence (k_0) of cyclophilin A. (C) Dependence of the relative amplitudes of the intermediate (◆) and slow phases (◇) upon cyclophilin A concentration. The *y*-axis represents the relative portion of the respective phase in the total amplitude of the two phases.

DISCUSSION

Structure of the Monomeric Folding Intermediate. The monomeric folding intermediate contains much of the native tertiary interactions as revealed by the fluorescence change during refolding (*12*). The increase of fluorescence intensity during refolding may represent the internalization of the tyrosine residues to form the hydrophobic active site. In addition to the hydrophobic active site, the monomeric folding intermediate may have hydrophobic surfaces to bind ANS (Figure 2). The hydrophobic surfaces would be utilized for making a contact with the partner molecule during dimerization. About 11% (∼670 Å) of the solvent-accessible area may be buried during dimerization per each monomer, in which the area was calculated by subtracting the area of dimer from those of two monomers based on the crystal

structure of *C. testosteroni* KSI (*3*). The exposure of hydrophobic residues can make the intermediate very unstable. The monomeric conformation appears to be much more unstable as the urea concentration increased as judged from the urea dependence analysis of the relative amplitudes of the refolding kinetic phases (Figure 4B). This might be related to the lower tendency of hydrophobic residues to internalize at higher urea concentrations.

The utilization of equilenin is a very sensitive way to monitor the formation of the active site since equilenin can bind to the active site very rapidly at the diffusion-controlled rate. The quenching of equilenin fluorescence at early stages, which accounted for approximately 40% of the total amplitude, implies that the hydrophobic active site might form rapidly (Figure 3). This is consistent with the abrupt fluorescence change observed in the fast phase that can originate only from the internalization of the active-site tyrosine residues into the hydrophobic environment. The rapid active-site formation in the burst phase may require the α-helices and β-sheet surrounding the active site to form at least partly. The ellipticity change at 225 nm during refolding revealed that more than 83% of the secondary structures might form in the burst phase during the dead time (*12*). This suggests that most native secondary structures might be generated prior to the internalization of the tyrosine residues. At the very early stage, KSI may form partly amphipathic α-helices, which may come together with the orientations of the hydrophobic side inward to surround the active site, resulting in the stable α-helices. From these results, it can be deduced that the monomeric folding intermediate has high contents of secondary and tertiary structures with the almost complete apolar active site and hydrophobic surfaces. The monomeric intermediate is nativelike, taking on most of the properties of the native protein, but less stable toward protein denaturation than the fully native protein since it has two hydrophobic areas inside and outside simultaneously.

Folding Mechanism. The fluorescence-detected folding kinetics of KSI can be described by three kinetic phases. The fast phase is a unimolecular process with the time range of $\tau_1 \sim 17-25$ ms. The urea-sensitive behavior of the fast phase indicates that this step may consist of one reaction of monomeric folding (Figure 4A). The intermediate and slow phases are responsible for the association process with time ranges of $\tau_2 \sim 10$ s and $\tau_3 \sim 60$ s, respectively. The dimerization contributes marginally to secondary structure formation but significantly to tertiary structure and active-site formation (*12*) (Figure 3). The rollover curvature of the urea dependence for the intermediate and slow steps suggests that these steps might involve more than one reaction and the rate-limiting step might change depending upon the urea concentration (Figure 4).

A simple sequential mechanism was proposed previously to explain KSI folding (*12*). In this mechanism, unfolded monomers (U) fold into the monomeric intermediates (I), and then they meet together to form the dimeric intermediate (I'_2). The dimeric intermediate may undergo further conformational rearrangements to form the native dimer (N_2). This mechanism is, however, inconsistent with the observation of the rollover curvature of the urea dependence of the rate constants for the intermediate and slow phases (Figure 4A). The catalysis of the intermediate and slow phases by cyclophilin A indicates the involvement of prolyl isomerizations as the rate-limiting step for these refolding phases (Figure 5). Thus, instead of the sequential mechanism, a sequential and parallel folding mechanism can be proposed based on the experimental evidence as depicted in Model 1,

Model 1

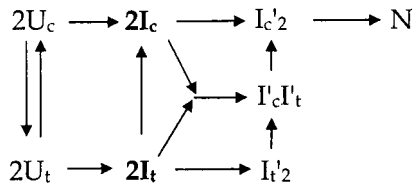

in which the subscripts c and t represent the cis and trans isomers of the Asp38−Pro39 peptide bond, respectively. The *C. testosteroni* KSI contains five proline residues per monomer, which are all in the trans configuration in the native state except the cis Asp38−Pro39 peptide bond. The proline isomerization might occur in the unfolded monomers or the folded monomeric intermediates before the association of monomers, or in the dimeric intermediates after association.

In Model 1, the fast reaction to form the monomeric folding intermediates, I_c and I_t, is likely to be indistinguishable spectroscopically. The cyclophilin A insensitive behavior of the fast reaction indicates that the reactions $U_c \rightarrow I_c$ and $U_t \rightarrow I_t$ may not be different in kinetic behavior. Given that the cis and trans imide bond linkages are typically 30% and 70% in population, respectively, in unstructured polypeptides (*26*), the monomeric intermediates, I_c and I_t, would also populate in a similar ratio to those of U_c and U_t. These monomeric intermediates, I_c and I_t, may associate with themselves to form $I_c'_2$ and $I_t'_2$, respectively, or with each other to form $I_c'I_t'$. The structural features at the dimeric interface require highly specific interactions between two convex β-sheets so that the different configurations of the Asp38−Pro39 peptide bond lying on strand 1 may affect the dimeric interactions. Actually, the dimeric interaction was so specific that it could be affected even by a single point mutation eliminating an intermolecular hydrogen bond (unpublished data, Nam and Choi). Thus, it would be expected that the reaction of $2I_c \rightarrow I_c'_2$, for which the peptide bond is in the same configuration as in the native state, may be more favorable than the other dimerization reactions. This dimerization step may be affected by the prolyl isomerization of the Asp38−Pro39 peptide bond, $I_t \rightarrow I_c$, and thus these steps together may constitute the intermediate phase.

This structural consideration also suggests that the slow phases might involve the reactions of both $I_c + I_t \rightarrow I_c'I_t'$ and $2I_t \rightarrow I_t'_2$. More effective catalysis of the slow phase than the intermediate phase by cyclophilin A reflects that the slow phase may be controlled more dominantly by prolyl isomerizations (Figure 5B). It is expected that the isomerization would be hard to occur in the dimeric state rather than in the monomeric state due to any structural constraints imposed on the dimeric state. Thus, the slow phase may be controlled by the slow isomerization reactions of $I_t'_2 \rightarrow I_c'_2$ and $I_c'I_t' \rightarrow I_c'_2$. Consistent with this speculation, cyclophilin A increased marginally the relative amplitude of the intermediate phase and decreased that of the slow phase (Figure 5C). This would likely be explained by the catalyzed prolyl

isomerization reaction, $I_t \rightarrow I_c$, resulting in the increase of the population of I_c. The similar dependence of the rate constants for both the intermediate and slow phases upon the urea concentration suggests that this mechanism can apply for the reactions at overall urea concentrations (Figure 4). Alternatively, the dependence of the intermediate phase on prolyl isomerizations might be due to non-native configurations of the imide bonds of Pro44 and Pro97 that will make the dimeric interaction unfavorable since these residues are located at the dimeric interface. Structural rearrangements originating from the unimolecular step of $I_c'_2 \rightarrow N_2$ may not be responsible for any significant change in fluorescence.

In conclusion, KSI folding involves the monomeric intermediate that might contain exposed hydrophobic surfaces and most of the native secondary structures. The KSI monomer intermediate is formed through the internalization of the apolar active-site residues to form the active site cavity. The dimerization may contribute significantly to the tertiary structure and active-site formation. The intermediate and slow phases are judged to involve both dimerization and proline isomerization reactions. Further characterization of the refolding process through mutational studies will enable a better understanding of the structural basis for the refolding mechanism of KSI. The analysis of NMR spectral features of the monomeric intermediate will also be valuable for understanding the intermediate structure and the folding mechanism in molecular detail.

REFERENCES

1. Batzold, F. H., Benson, A. M., Covey, D. F., Robinson, C. H., and Talalay, P. (1976) *Adv. Enzyme Regul. 14*, 243−267.
2. Benson, A. M., Jarabak, J., and Talalay, P. (1971) *J. Biol. Chem. 246*, 7514−7525.
3. Cho, H.-S., Choi, G., Choi, K. Y., and Oh, B.-H. (1998) *Biochemistry 37*, 8325−8330.
4. Wu, Z. R., Ebrahimian, S., Zawrotny, M. E., Thornburg, L. D., Perez-Alvarado, G. C., Brothers, P., Pollack, R. M., and Summers, M. F. (1997) *Science 276*, 415−418.
5. Kraulis, P. J. (1991) *J. Appl. Crystallogr. 24*, 946−950.
6. Lundqvist, T., Rice, J., Hodge, C. N., Basarab, G. S., Pierce, J., and Lindqvist, Y. (1994) *Structure 2*, 937−944.
7. Bullock, T. L., Clarkson, W. D., Kent, H. M., and Stewart, M. (1996) *J. Mol. Biol. 260*, 422−431.
8. Kim, S. W., Cha, S.-S., Cho, H.-S., Kim, J.-S., Ha, N.-C., Cho, M.-J., Joo, S., Kim, K.-K., Choi, K. Y., and Oh, B.-H. (1997) *Biochemistry 36*, 14030−14036.
9. Murzin, A. G. (1998) *Curr. Opin. Struct. Biol. 8*, 380−387.
10. Kuliopulos, A., Shortle, D., and Talalay, P. (1987) *Proc. Natl. Acad. Sci. U.S.A. 84*, 8893−8897.
11. Kim, S. W., Kim, C. Y., Benisek, W. F., and Choi, K. Y. (1994) *J. Bacteriol. 21*, 6672−6676.
12. Kim, D.-H., Jang, D. S., Nam, G. H., Yun, S., Cho, J. H., Choi, G., Lee, H. C., and Choi, K. Y. (2000) *Biochemistry 39*, 13084−13092.
13. Gloss, L., and Matthews, C. R. (1998) *Biochemistry 37*, 15990−15999.
14. Gloss, L., and Matthews, C. R. (1998) *Biochemistry 37*, 16000−16010.
15. Wallace, L. A., and Dirr, H. W. (1999) *Biochemistry 38*, 16686−16694.
16. Waley, S. G. (1973) *Biochem. J. 135*, 165−172.
17. Zabori, S., Rudolph, R., and Jaenicke, R. (1980) *Z. Naturforsch. 35C*, 999−1004.
18. Milla, M. E., Brown, B. M., Waldburger, C. D., and Sauer, R. T. (1995) *Biochemistry 34*, 13914−13919.
19. Ptitsyn, O. B., Pain, R. H., Semisotnov, G. V., Zerovnik, E., and Razgulyaev, O. I. (1990) *FEBS Lett. 262*, 20−24.
20. Semisotnov, G. V., Rodionova, N. A., Razgulyaev, O. I., Uversky, V. N., Gripas, A. F., and Gilmanshin, R. I. (1991) *Biopolymers 31*, 119−128.
21. Kim, D.-H., Nam, G. H., Jang, D. S., Choi, G., Joo, S., Kim, J.-S., Oh, B.-H., and Choi, K. Y. (1999) *Biochemsitry 38*, 13810−13819.
22. Copeland, R. A. (1993) in *Methods of protein analysis*: *a practical guide to laboratory protocols*, Chapman and Hall, New York.
23. Cho, H.-S., Ha, N.-C., Choi, G., Kim, H.-J., Lee, D., Oh, K. S., Kim, K. S., Lee, W., Choi, K. Y., and Oh, B.-H. (1999) *J. Biol. Chem. 274*, 32863−32869.
24. Hawkinson, D. C., Pollack, R. M., and Ambulos, N. P., Jr. (1994) *Biochemistry 33*, 12172−12183.
25. Massiah, M. A., Abeygunawardana, C., Gittis, A. G., and Mildvan, A. S. (1998) *Biochemistry 37*, 14701−14712.
26. Brandts, J. F., Halvorson, H. R., and Brennan, M. (1975) *Biochemistry 14*, 4953.

BI0019139